

Field Emission Properties of Carbon nanotubes Coated with Boron Nitride

Noejung Park,^a Seungwu Han,^b and Jisoon Ihm^{a,*}

^a*School of Physics, Seoul National University, Seoul 151-742, Korea*

^b*Princeton Material Institute, Princeton University, Princeton, New Jersey, USA*

In honor of Prof. Dr. Jürgen Pebler's 65th birthday

Field emission properties of carbon nanotubes coated with a single layer of boron nitride are calculated using the first-principles pseudopotential method. At lower bias voltage, the emission current of the coated nanotube is comparable to that of the bare carbon nanotube and is dominated by the contribution from localized states at the tip of the tube. At higher voltage, newly generated hybridized states between the carbon nanotube tip and the even-membered boron nitride rings contribute significantly to the emission current because they experience a low tunneling barrier compared with the bare carbon nanotube case. Our results suggest that the insulator coating can, besides protecting the nanotube tip from the attack of gas molecules, substantially enhance the field emission current.

Keywords:

1. INTRODUCTION

The carbon nanotube (CNT) has been considered to be an ideal material for field emitters because of its exceptionally high aspect ratio and chemical stability. Numerous experimental studies have reported that CNT field emitters have a low threshold voltage and large current density.^{1–4} Theoretical studies have revealed the importance of the localized states,⁵ the advantages of the open tube over the closed one,^{6,7} and the enhancement in the emission current by gas adsorbates.^{8,9}

One of the important issues to be resolved in the manufacture of nanotube-based field emission displays (FEDs) is the stability of the emission current under ambient gases. Although the current of the nanotube field emitter is shown to be more stable than that of a micron-sized metal tip in a low current condition,¹⁰ “long-time degradation” under a moderate vacuum condition¹¹ still exists in CNT field emitters. Since an ultrahigh vacuum is hard to implement in practical device operations, such an irreversible degradation could be an obstacle to commercialization of nanotube-based FEDs.

In the case of micrometer-sized metal tips, substantial degradation in the emission current in an oxygen or water environment¹² has been known and is a primary reason why these field emitters cannot be used in practice. Furthermore, the tip of the emitter is bombarded severely by positively ionized molecules under an extremely high

local field at the tip region. Some authors have tried to overcome these shortcomings by coating the emitting surface with hard semiconducting materials. The coated surface turns out to be less sensitive to the vacuum condition.¹³ In addition, owing to the small electron affinity at the outer semiconducting surface, the barrier for electron emission is effectively lowered from that of the bare metal surface.¹⁴

In conceptual analogy to the coated metal-tip emitters, we propose in this work a CNT coated with boron nitride as a nanoscale emitter that can provide both long-term stability and large emission current. As boron nitride is known to be more stable upon oxygen adsorptions than carbon nanotubes,^{15,16} the coated nanotube is not likely to be damaged by oxidative etching and, consequently, would not show a long-time irreversible degradation in the emission current. However, since the emission mechanism in the nanotube is quite different from that of microtips, it is questionable whether a nanotube can be coated without losing its advantages as an electron emitter, for example, the existence of localized states and strong field enhancement at the end of the tube. To answer this question, we perform three-dimensional first-principles calculations on model geometries of the coated nanotube. Our calculational results show that, in addition to the protecting effects against gas adsorption, the boron nitride coating can induce an increase in the emission current over that of the bare CNT.

*Author to whom correspondence should be addressed.

Calculational methods employed in this work are described in the next section. Model geometries and calculated emission currents are presented in Section 2.2. Detailed investigations of the electronic structures of the coated nanotubes are given in Section 2.3. Results are summarized in the last section.

2. EXPERIMENTAL DETAILS

2.1. Calculational Method

Electronic structures and equilibrium geometries are calculated with the first-principles pseudopotential method.¹⁷ The local density approximation is employed for the exchange-correlation potential.¹⁸ The pseudopotential is generated through the Troullier-Martins scheme,¹⁹ and its nonlocal part is converted into the fully separable form of Kleinman and Bylander.²⁰ To deal with a large system we use the atomic-orbital-type localized basis set. The numerical basis set for pseudo-atomic orbitals (one *s* and three *p* orbitals per atom) is generated by the method of Sankey and Niklewski.²¹ The calculation of the emission current is based on the two-step process.²² First, the electronic structure and the potential under the external voltage are calculated self-consistently with the localized basis. Next, the basis set is switched to the plane waves, and the tunneling rate of the electron into the vacuum region is calculated by solving the time-dependent Schrödinger equation.

2.2. Model Geometry and Field Emission Current

To investigate the effect of boron nitride coating on CNT field emitters, we construct two model geometries for coated nanotubes. Figure 1a is a schematic illustration of the coated nanotubes. Here we assume that only the top-most part of the CNT is coated with a boron nitride layer (represented by thick the line) for computational convenience. In Figure 1b, the side view of an actual atomic configuration of a closed (5, 5) CNT (lower part) and the top view of the cap of the (10, 10) boron nitride nanotube (lower part) are shown. Hereafter we call this model geometry the Type-I coated nanotube. The cap part of the boron nitride nanotube has three square rings.²³ The CNT is closed with a hemisphere of C₆₀ preserving the fivefold rotational symmetry with respect to the tube axis. The total length of the CNT used in the calculation is about 35 Å. The geometry of the boron nitride cap and the CNT are independently optimized with first-principles calculations. The distance between the boron nitride cap and the CNT is set at 3.3 Å. In Figure 1c, the open (4, 4) CNT coated with the cap of the (8, 8) boron nitride nanotube is shown. This model geometry is called the Type II coated nanotube hereafter. The boron nitride cap, in this case, has four squares and one octagon. Because of the heavy computational load of the first-principles method, thicker

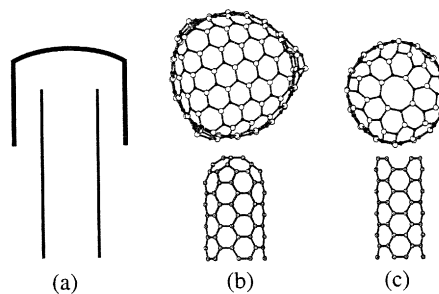


Fig. 1. Model geometries for a carbon nanotube coated with a single layer of boron nitride. (a) Schematic illustration for the side view of the coated nanotube. (b) Top view of the (10, 10) boron nitride nanotube cap and the side view of the closed (5, 5) carbon nanotube. (c) Top view of the (8, 8) boron nitride nanotube cap and side view of the open (4, 4) carbon nanotube. For visual clarity, the boron nitride cap and the body of the carbon nanotube are shown separately. Three boron nitride square rings are present in (b), and four square rings and one octagon ring are present in (c).

layers of the boron nitride coating are not considered in the present study.

Field emission currents of each model geometry under external fields ranging from 0.3 V/Å to 0.7 V/Å are calculated. Since the length of the nanotube in the calculation is much shorter than that of the experiment and thus the field enhancement factor is much smaller, a large applied field is required in the calculation to simulate the actual local electric field around the tip in the experiments⁵ (typically 0.5–1.5 V/Å). To calculate the time-evolved electronic states properly, we need a large vacuum in the unit cell. In this calculation the vacuum region in the supercell is about 30 Å long in the axial direction, and the tunneling rate of the electron to the vacuum is calculated before the front of the emitted electron reaches the cell boundary. The intertube separation in a direction perpendicular to the tube axis is made as large as 28 Å to reduce the undesired interactions between the neighboring tubes.

Calculated emission currents of each model system are shown in Figure 2. The *I*–*V* curves (when $E_{\text{ext}} \geq 0.5$ V/Å, in the case of Type I a linear behavior in the Fowler-Nordheim plot.²⁴ The magnitude of the current, which is in the range of a few tenths of nanoamperes to several microamperes, is consistent with the experiment.¹⁰ An interesting result in this figure is that the emission current from the coated nanotube is larger than that of the bare carbon nanotube. In the Type I tube, the current of the coated nanotube and that of the bare nanotube are comparable in the low field condition. However, in the high field condition, the current in the coated nanotube is larger than that of the bare carbon nanotube by two orders of magnitude. In the Type II tube, there is enhancement of the emission current in the high field, but it is small (Fig. 2b). To understand the reason for the current increase by the boron nitride coating, we investigate the characteristics of the dominantly emitting states in detail in the next section.

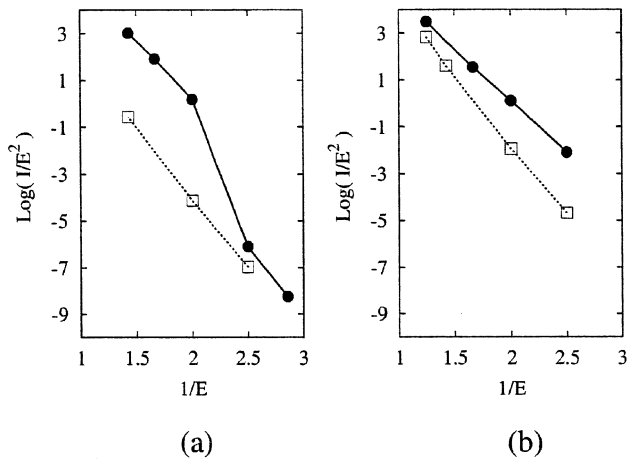


Fig. 2. Fowler-Nordheim plots²⁴ for the emission current of (a) the Type I coated nanotube and the bare (5, 5) carbon nanotube and (b) the Type II coated nanotube and the bare (4, 4) carbon nanotube. The solid circles represent the calculated values for the coated nanotubes, and the open squares represent those of the bare carbon nanotubes. The emission current I is in μA and the electric field E is in $\text{V}/\text{\AA}$.

2.3. Local Electronic Structure of the Coated nanotube

Now we present the local electronic structures at the tip of each model geometry. The local density of electronic states (LDOS) of the Type I coated nanotube is shown in Figure 3a. The upper part of the figure corresponds to the case without external fields, and the lower part corresponds to the case with the external field $E_{\text{ext}} = 0.5 \text{ V}/\text{\AA}$. The LDOS for the five topmost carbon atoms (pentagonal ring) at the CNT cap is plotted as a solid line and that for the boron nitride cap (116 atoms) is plotted by a dotted line. The peak indicated by A represents doubly degenerate states strongly localized at the cap of the CNT; one of them is symmetric with respect to a mirror plane of the CNT and the other is antisymmetric.¹⁸

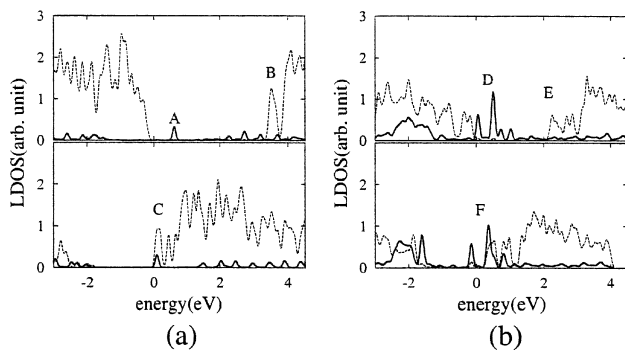


Fig. 3. LDOS for the tip of the carbon nanotubes and the boron nitride caps. Solid lines in (a) represent the LDOS for the five topmost carbon atoms at the cap of the carbon nanotube, and those in (b) represent the LDOS for the eight carbon atoms at the armchair edge. Dotted lines represent the LDOS for the boron nitride cap for both (a) and (b). The upper parts are for the cases without external fields, and the lower parts are with the external field $E_{\text{ext}} = 0.5 \text{ eV}$.

These doubly degenerate states contribute dominantly to the field emission of the bare CNT ($\sim 75\%$). On the other hand, low-lying conduction bands of the boron nitride cap around 4 eV are nonbonding states of p_z orbitals of boron atoms.²⁵ In particular, the states indicated by B in Figure 3a are the localized states at the square rings. These square rings are located at the corner of the flat cap geometry of the boron nitride tube. The large curvature in this region induces a significant σ - π hybridization in the localized states, and these states shift down with respect to pure nonbonding p_z states.

Under large external fields ($\geq 0.5 \text{ V}/\text{\AA}$), localized states in the boron nitride cap shift down and are hybridized with the localized states in the CNT, as shown in the lower part of Figure 3a. Most of the emission current comes from the hybridized states. For example, when $E_{\text{ext}} = 0.5 \text{ V}/\text{\AA}$, the hybridized states emit a current that is 70 times larger than that of the localized states in the bare CNT. The fact that the hybridized states provide much larger current than the bare CNT states is ascribed to the reduced electron affinity by boron nitride coating. Since low-lying conduction bands of the boron nitride cap (indicated by B in Fig. 3a) are located 3 eV higher than the localized CNT states (indicated by A in Fig. 3a), the electron affinity of the hybridized state under the external field should be smaller than that of the bare CNT. In other words, the tunneling barrier for the hybridized states is lower and narrower than that for the localized states of the bare CNT. As will be explained in the last part of this section, the decreased slope in the Fowler-Nordheim plot for the coated nanotube can be interpreted as a reflection of the reduced electron affinity.

In Figure 3b, the LDOS for the top eight carbon atoms forming the armchair edge is shown by a solid line, and that of the boron nitride cap (56 atoms) is shown by a dotted line. In this case, the bonding states of the dangling bond orbitals of the armchair edge form the peaks around -2.0 eV , and the antibonding states of those orbitals form two peaks, indicated by D; the smaller peak at 0.1 eV represents a nondegenerate state, and the larger peak at 0.57 eV represents doubly degenerate states. As in the case of the Type I nanotube, localized states in the even-membered boron nitride rings form low-lying states of the conduction bands. In particular, states indicated by E are very strongly localized at the flat cap with a large weight in the octagon (to be shown in Fig. 4b). Four p_z orbitals of the boron atoms in the octagon form antibonding states without hybridization with σ -states. We designate this state as the octagon state. The octagon state is orthogonal to π and π^* states of the CNT because it has a different reflection symmetry with respect to a mirror plane of the nanotube. Under the external field, the localized states in the boron nitride cap shift down and are hybridized with the dangling-bond states of the CNT, as shown in the lower part of Figure 3b. The octagon state

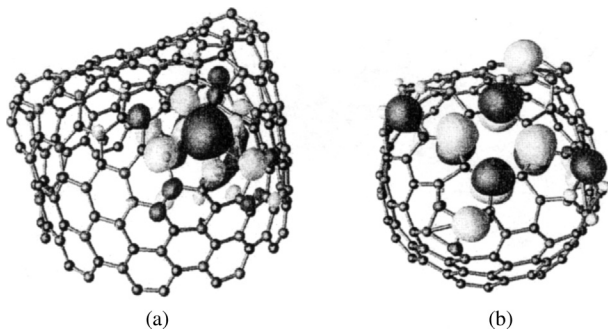


Fig. 4. Plot of the wavefunction illustrating the localization of the state (a) at the square boron nitride rings of the (10, 10) boron nitride cap and that (b) at the square and octagon rings of the (8, 8) boron nitride cap. The red and yellow colors indicate positive and negative signs of the wavefunction, respectively.

does not form a bond with the π or π^* states because of different symmetry.

In the previous figure (Fig. 2b), we present a comparison between the emission current of the bare CNT and that of the coated nanotube. Since the dangling-bond states are known to be the best emitting state in the clean graphitic edge,²⁶ the fact that the coated nanotube gives larger current than the open CNT with dangling bonds is rather surprising. In this case, the calculated field strength for inducing the hybridization between CNT states and boron nitride cap states is lower than the field range shown in Figure 2, and, consequently, the hybridized states dominate the emission current of the coated nanotube over the whole field range studied (hence there no abrupt change in the slope of the solid line). The reduced slope of the coated nanotube in Figure 2b may be interpreted as the reduced electron affinity as follows. In the one-dimensional analysis with the WKB approximation, the slope in the Fowler-Nordheim plot is proportional to $\phi^{3/2}/\beta$, where ϕ is the work function (or electron affinity in the present case) and β is the field enhancement factor. Although our calculational method is a full quantum mechanical three-dimensional one, the I - V plot of each electronic state shows the Fowler-Nordheim behavior to a good approximation. Since the field enhancement factor β does not increase by boron nitride coating, the smaller slope of the coated nanotube shown in Figure 2 can be interpreted as a manifestation of the reduced electron affinity. Finally, we plot the wavefunction of the localized states in Figure 4 to help visualize the characteristic feature of the localized states contributing dominantly to the emission current. Figure 4a shows the wavefunction of the state localized at the square boron nitride rings of the (10, 10) boron nitride cap, and Figure 4b shows the state localized at the square and octagon rings of the (8, 8) boron nitride rings.

Although the localized state in the model system stems from the presence of even-membered boron nitride rings, the localized state commonly exists at the tip of an atomistically sharp material. Therefore, the advantages in coat-

ing the carbon nanotube with large gap material could be applied to broader situations. To achieve a coating thickness of less than a few atomic layers, a novel coating method is required. The synthesis technique leading to double-walled nanotubes seems to be promising in this respect.

3. CONCLUSIONS

We have investigated the field emission characteristics of carbon nanotubes coated with a single layer of boron nitride. The emission current from the coated nanotube is found to be larger than that of the bare carbon nanotube. The increase in the emission current is mostly ascribed to the reduction of the electron affinity induced by the boron nitride coating. Considering the experimentally known good stability of field emission of the boron nitride nanotube,²⁷ the boron nitride-coated carbon nanotube can potentially be a better emission tip with an increased emission stability and a larger emission current than the bare carbon nanotube.

Acknowledgments: This work was supported by the Center for nanotubes and Nanostructured Composites of Sungkyunkwan University and the BK21 Project. The computation by supercomputers was supported by the Korea Institute of Science and Technology Information.

References and Notes

1. Q. H. Wang, T. D. Corrigan, J. Y. Dai, R. P. H. Chang, and A. R. Krauss, *Appl. Phys. Lett.* 70, 3308 (1997).
2. W. Zhu, C. Bower, O. Zhou, G. Kochanski, and S. Jin, *Appl. Phys. Lett.* 75, 873 (1999).
3. J. M. Bonard, F. Maier, T. Stockli, A. Chatelain, W. A. de Heer, J. P. Salvetat, and L. Forro, *Ultramicroscopy* 73, 7 (1998).
4. K. A. Dean and B. R. Chalamala, *Appl. Phys. Lett.* 75, 3017 (1999).
5. S. Han and J. Ihm, *Phys. Rev. B* 61, 9986 (2000).
6. Ch. Adessi and M. Devel, *Phys. Rev. B* 62, R13314 (2000).
7. G. Zhou, W. Duan, and B. Gu, *Phys. Rev. Lett.* 87, 95504 (2001).
8. N. Park, S. Han, and J. Ihm, *Phys. Rev. B* 64, 125401 (2001).
9. A. Maiti, J. Andzelm, N. Tanpipat, and P. v. Allmen, *Phys. Rev. Lett.* 87, 155502 (2001).
10. K. A. Dean and B. R. Chalamala, *Appl. Phys. Lett.* 76, 375 (2000).
11. K. A. Dean and B. R. Chalamala, *Appl. Phys. Lett.* 75, 3017 (2000).
12. B. R. Chalamala, R. M. Wallace, and B. E. Gnade, *J. Vac. Sci. Technol., B* 16, 2859 and 17, 303 (1998).
13. J. L. Shaw, H. F. Gray, K. L. Jenson, and T. M. Jung, *J. Vac. Sci. Technol., B* 14, 2072 (1996).
14. V. T. Binh and Ch. Adessi, *Phys. Rev. Lett.* 85, 864 (2000).
15. T. Sugino, and S. Tagawa, *Appl. Phys. Lett.* 74, 889 (1999).
16. W. Han, Y. Bando, K. Kurashima, and T. Sato, *Jpn. J. Appl. Phys.* 38, 755 (1999).
17. J. Ihm, A. Zunger, and M. L. Cohen, *J. Phys. C* 12, 4409 (1979).
18. D. M. Ceperley and B. J. Alder, *Phys. Rev. Lett.* 45, 566 (1980).
19. N. Troullier and J. L. Martins, *Phys. Rev. B* 43, 1993 (1991).
20. L. Kleinman and D. M. Bylander, *Phys. Rev. Lett.* 48, 1425 (1982).
21. O. F. Sankey and D. J. Niklewski, *Phys. Rev. B* 40, 3979 (1989).

22. S. Han, M. H. Lee, and J. Ihm, *Phys. Rev. B* 65, 085405 (2002).
23. G. Golberg, W. Han, Y. Bando, L. Bourgeois, K. Kurashima, and T. Sato, *J. Appl. Phys.* 86, 2364 (1999).
24. R. H. Fowler and L. Nordheim, *Proc. R. Soc. London, Ser. A* 119, 173 (1928).
25. N. Park, C. Cho, and J. Ihm, unpublished observations.
26. K. Tada and K. Watanabe, *Phys. Rev. Lett.* 88, 127601 (2002).
27. J. Cumings and A. Zettl, in *Electronic Properties of Molecular Nanostructures*, edited by H. Kuzmany, American Institute of Physics, New York (2001), p. 577.

Received: 30 July 2002. Revised/Accepted: 6 March 2003.